5th Australasian Congress on Applied Mechanics, ACAM 2007
10-12 December 2007, Brisbane, Australia

A theory of strongly orthotropic continuum mechanics

D.C. Kellermann and T. Furukawa

School of Mechanical and Manufacturing Engineering, the University of New South Wales, Sydney, NSW 2052, Australia

Abstract: This paper presents a theory of continuum mechanics for strongly orthotropic materials that proposes a more informative asymmetric strain and rotation tensor. The infinitesimal strain tensor and, likewise, Green-Lagrange strains avoid rotational sensitivity by the use of effective shear strain averaging. The linear formulation of the proposed non-symmetric strain tensor field instead differentiates planar shear strains based on principal material direction and mechanical properties – adding determinacy to the otherwise geometric problem. The separation of in-plane shears also allows the formulation of a first order rotation tensor that gives change in principal property direction when applied to orthotropic materials – which is a new interpretation of rigid body rotation. Subsequent to the theory, a new extended Mohr's plot and compliance tensor are presented. It is demonstrated in a numerical example that application of the proposed tensors yields the best solution when compared with an analytical model and three conventional solvers for a finite shear deformation.

Keywords: strongly orthotropic, asymmetric strain tensor, rotation tensor, continuum mechanics

1 Introduction

Strongly orthotropic materials such as continuous fibre reinforced composites exhibit directional behaviour and thus provide more capabilities for mission and application tailored design than regular isotropic materials. The directional properties introduced by their anisotropic makeup, however, complicate their deformation and further the assumptions required for continuum mechanics analysis. A number of issues stem from the use of symmetric strain tensors, derived for isotropic media [1, 2], that are necessitated by the requirement for insensitivity to small rigid body rotation [3]. Without the averaging of in-plane shear terms, there exist an infinite number of compatible modes for any distorted state. Affected by this in particular, strongly orthotropic materials magnify an associated second order error under finite deformation due to the relatively inextensible nature of the fibres.

Significant recent attention has been directed towards this strongly orthotropic class of materials: Boisse [4], in eliminating any such continuum assumptions, used a multi-scale approach to accurately model sub-structural response of woven fibre composites in forming; although this came with the associated computational expense. By instead treating individual fibre families in their own material coordinate systems, and by using the kinematic assumptions developed by Spencer [5], Xu et al [6] were able to decompose and tailor the strain tensor to an associated constitutive model. This approach, whilst being kinematically improved, could not encompass the effect of a matrix component comparable in stiffness to the fibres. In simulating this particular forming problem, the most practical method was developed by Yu et al [7], whose investigative efforts concluded that a simple remedy was to strictly align meshes with material orientation. Whilst also solving numerical locking problems, this method allowed the material response to be mapped directly against experimental results, thus usurping the need for involved tensorial treatment. This, nonetheless, could not be considered a continuum mechanics solution, and required significant empirical data. In modelling similar materials, including structurally reinforced elastomeric materials, recent work by Nedjar [8] addressed these same issues by the use of structural tensors. Building on developments largely by Klinkel [9], this formulation allowed the projection components of deformation to be treated uniquely for any number of fibre families. Effectively, this and the various aforementioned efforts have treated material coordinates as being pinned to fibre direction, thus the commonality has been to treat the materials not as strongly, but *infinitely* orthotropic in terms of deformation modality. Thus there remains an error associated with any orthotropic material under finite distortive strain that has not yet been addressed.

This paper presents a continuum mechanics basis that models the asymmetric strain state and material principal rotation continuously from isotropy to strongly orthotropic material. This is based on the postulation of asymmetrically equilibrated yet determinate strain states using dependency on the material orientation and mechanical properties. This, the so called *Orthotropic Linear Strain Tensor*

(OLST), is also used to derive a first order rotation tensor that gives change in material principal direction rather than geometric rigid body rotation. The problems of non-orthonormal basis vectors, following large shear deformation, for materials with inherent principal directionality are avoided by the use of persistently orthotropic material coordinate systems. These concepts are used to reformulate the necessary parts for a 2D analysis using the proposed strain tensors and transformation matrices.

The paper is organised as follows: In section 2, notation and the conventional linear strain tensor is presented. Following this, key concepts and techniques relating to the proposed theory are introduced. This is used, in the section that follows, for a numerical example demonstrating the benefits of the proposed concepts. The final section draws conclusions regarding the work presented.

2 The linear tensors of the displacement state

The strain tensor $\mathbf{e}$ is referred to as the *Isotropic Linear Strain Tensor* (ILST), in planar form this is:

$$^{\{m\}}\mathbf{e} = \left\{e_{11} \quad e_{22} \quad e_{12}\right\}^{\mathrm{T}}, \quad ^{\{g\}}\mathbf{e} = \left\{e_{xx} \quad e_{yy} \quad e_{xy}\right\}^{\mathrm{T}} \tag{1}$$

When numeric indices are used, the values are in the local material coordinate system m, and when Roman minuscule letters are used, the values are in any arbitrary global coordinate system g. Using the displacement gradient $\nabla\mathbf{u}$, the linear strain tensor field can be expressed as

$$\mathbf{e} = \left(\overleftarrow{\nabla}\mathbf{u} + \overrightarrow{\nabla}\mathbf{u}\right)\big/2, \quad e_{ij} = \left(u_{i,j} + u_{j,i}\right)\big/2 \tag{2}$$

with components shown in index notation, and noting that commas between indices infer the spatial derivative. If we remove the assumption of symmetry, whereby

$$e_{yx} = e_{xy}, \quad D_{1212} = D_{2121}, \tag{3}$$

then the knowledge of the strain state is reduced to:

$$e_{ij} + e_{ji} = u_{i,j} + u_{j,i}. \tag{4}$$

By considering the linear strain tensor is actually the symmetric part of the displacement gradient, the residual tensor, rigid body rotation ω, is given by the skew symmetric component:

$$\omega_{i\times j} = \left(u_{j,i} - u_{i,j}\right)\big/2 \tag{5}$$

where the use of the cross product in the indices is such that $\omega_{i\times j} = \omega_k$.

3 Continuum mechanics using the strongly orthotropic postulate

3.1 Derivation of the orthotropic linear strain tensor

In order to derive the OLST field, we first define the vectorized tensor, differing from (1): the ILST in Voigt notation. Because an *orthotropic* linear strain tensor with values unique to the ILST is to be defined, the denotation $\boldsymbol{\text{œ}}$ is used rather than $\mathbf{e}$:

$$^{\{m\}}\boldsymbol{\text{œ}} = \left[æ_{11}, æ_{22}, æ_{12}, æ_{21}\right]^{\mathrm{T}}, \quad ^{\{g\}}\boldsymbol{\text{œ}} = \left[æ_{xx}, æ_{yy}, æ_{xy}, æ_{yx}\right]^{\mathrm{T}} \tag{6}$$

where (4) now applies such that $æ_{ij} + æ_{ji} = u_{i,j} + u_{j,i}$. Based on the postulation, the proposed strain tensor is, unlike the ILST, dependent on the material property set including the fourth-order elasticity tensor, $\mathbf{D}$, and the angle to the material principal direction, $\boldsymbol{\theta}$:

$$^{\{g\}}\boldsymbol{\text{œ}} = f\left(^{\{g\}}\nabla\mathbf{u}, {}^{\{m\}}\mathbf{D}, {}^{\{g\}}\boldsymbol{\theta}\right) \tag{7}$$

We omit the simplification whereby shear strains are assumed equal, as in the ILST and (3), and therefore the planar elasticity tensor takes the form:

$$^{\{m\}}\mathbf{D} = \begin{bmatrix} D_{1111} & D_{1122} & & \cdots 0 \cdots \\ D_{2211} & D_{2222} & & \\ & \cdots 0 \cdots & D_{1212} & 0 \\ & & 0 & D_{2121} \end{bmatrix} \tag{8}$$

Adhering to the well known form, stress and the orthotropic strain tensor are related by the fourth order tensor of Eq (8) and similarly in any global coordinate frame, whereby the global stiffness matrix should be a function of the material local stiffness matrix:

$$^{\{m\}}\boldsymbol{\sigma}^{\text{œ}} = {}^{\{m\}}\mathbf{D}\,{}^{\{m\}}\boldsymbol{\text{œ}}, \quad {}^{\{g\}}\boldsymbol{\sigma}^{\text{œ}} = {}^{\{g\}}\mathbf{D}\left({}^{\{m\}}\mathbf{D}, \boldsymbol{\theta}\right){}^{\{g\}}\boldsymbol{\text{œ}} \tag{9}$$

The required global strain and stress matrices are given by:

$$^{\{g\}}\boldsymbol{\text{œ}} = \mathbf{T}\,{}^{\{m\}}\boldsymbol{\text{œ}}, \quad {}^{\{g\}}\boldsymbol{\sigma}^{\text{œ}} = \mathbf{T}\,{}^{\{m\}}\boldsymbol{\sigma}^{\text{œ}} \tag{10}$$

using the transformation matrix $\mathbf{T}$, derived using the transformation law $œ_{ij}$' = $l_{ip}l_{jq}œ_{pq}$; noting the Einstein summation convention for free indices, and the direction cosines l_{ij}. The required material matrix in the global coordinate system, adopting potential shear coupling terms, is found using $^{\{g\}}\mathbf{D} = \mathbf{T}^{-1}\,{}^{\{m\}}\mathbf{D}\mathbf{T}$. The subsequent global model of (9) is thus defined by ten unique functions:

$$\begin{Bmatrix} \sigma_{xx}^{\text{œ}} \\ \sigma_{yy}^{\text{œ}} \\ \sigma_{xy}^{\text{œ}} \\ \sigma_{yx}^{\text{œ}} \end{Bmatrix} = \begin{bmatrix} f_1\left({}^{\{m\}}\mathbf{D},\boldsymbol{\theta}\right) & f_9\left({}^{\{m\}}\mathbf{D},\boldsymbol{\theta}\right) & f_8\left({}^{\{m\}}\mathbf{D},\boldsymbol{\theta}\right) & f_7\left({}^{\{m\}}\mathbf{D},\boldsymbol{\theta}\right) \\ & f_2\left({}^{\{m\}}\mathbf{D},\boldsymbol{\theta}\right) & f_{10}\left({}^{\{m\}}\mathbf{D},\boldsymbol{\theta}\right) & f_6\left({}^{\{m\}}\mathbf{D},\boldsymbol{\theta}\right) \\ & & f_3\left({}^{\{m\}}\mathbf{D},\boldsymbol{\theta}\right) & f_5\left({}^{\{m\}}\mathbf{D},\boldsymbol{\theta}\right) \\ \cdots sym \cdots & & & f_4\left({}^{\{m\}}\mathbf{D},\boldsymbol{\theta}\right) \end{bmatrix} \begin{Bmatrix} œ_{xx} \\ œ_{yy} \\ œ_{xy} \\ œ_{yx} \end{Bmatrix} \tag{11}$$

Notably, these functions reduce to conventional transformations if the omitted condition (3) is included.

The stress tensor in the global coordinate system must maintain the in-plane moment equilibrium implied by the ILST; thus in shear $\sigma_{xy}^{\text{œ}} = \sigma_{yx}^{\text{œ}}$. The assembly of this equality with (11) and the condition equivalent to (4) define the first shear strain term:

$$œ_{xy} = \left\{(f_8 - f_7)u_{x,x} + (f_{10} - f_6)u_{y,y} + (f_5 - f_4)(u_{x,y} + u_{y,x})\right\} \big/ (2f_5 - f_3 - f_4) \tag{12}$$

Note that the second shear strain term is found by an identical process. By substitution of the transformation functions, the proposed orthotropic strain tensor field can be explicitly expressed for the two-dimensional case, which is written compactly by:

$$œ_{ij} = \left(u_{i,j} + u_{j,i}\right)\left(d_{ij}\sin^2\theta_{ij} + d_{ji}\cos^2\theta_{ij}\right) + \left(u_{i,i} - u_{j,j}\right)\frac{d_{ij} - d_{ji}}{2}\sin 2\theta_{ij} \tag{13}$$

where we define the *balance ratio* as: $d_{ij} = D_{ijij} \big/ \left(D_{ijij} + D_{jiji}\right), \forall D \in m^3$ and where θ_{ij} refers to the projected component of the fibre angle in the plane of measurement indicated such that $\theta_{ij} = -\theta_{ij}$. As a demonstration of the universal applicability of the formulation, we see that under the hitherto omitted equality of (3), (13) easily reduces to $œ_{xy} = (u_{x,y} + u_{y,x})/2$; which is identical to the ILST as shown in (2).

Based on the same relationship between (2) and (5), the proposed material principal rotation tensor can similarly be found from (13):

$$\psi_{i\times j} = u_{j,i}\left(d_{ij}\sin^2\theta_{ij} + d_{ji}\cos^2\theta_{ij}\right) - u_{i,j}\left(d_{ji}\sin^2\theta_{ji} + d_{ij}\cos^2\theta_{ji}\right) + \left(u_{i,i} - u_{j,j}\right)\frac{d_{ij} - d_{ji}}{2}\sin 2\theta \tag{14}$$

Note that all generalised tensor and indicial forms are applicable to the three dimensional case providing the material coordinate system is only rotated in one plane.

3.2 The Extended Mohr's Plot for the orthotropic strain tensor

Considering the proposed tensors in (13) and (14), we introduce a metric for their *aspectual strain* $\boldsymbol{\alpha}$ to describe the latter part of the formula. This has components: $\alpha_{ij} = (u_{i,i}-u_{j,j})/2$ which produce a positive value when the aspect ratio increases, a negative value for a decrease, and no change for pure planar dilatation strain. At 45° to the maximum shear orientation, where the shear component diminishes to zero, pure aspectual strain represents deviatoric change only.

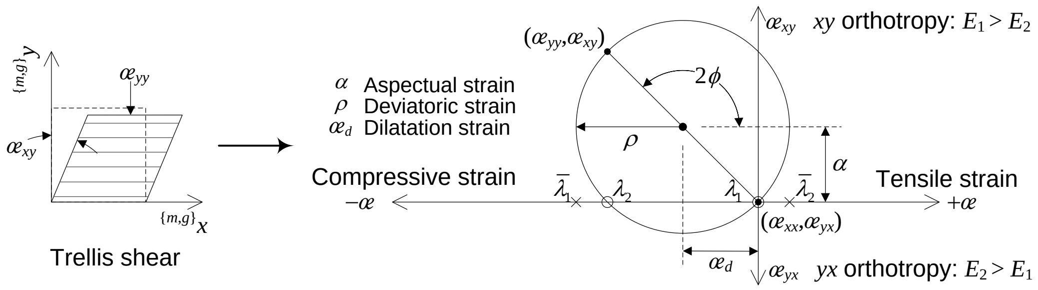

Figure 1. Characteristic strain indicators of the proposed extended Mohr's plot, unbound from the horizontal axis

In Figure 1 an example of the proposed Extended Mohr's Plot is shown for the trellis motion of an infinitely orthotropic material with a fibre angle of $\theta_{xy} = 0$, where $d_{xy} = 1$ such that $æ_{yx} = 0$. As with a conventional Mohr's plot for strain, ϕ represents the angle between the measured global coordinate system and the horizontal orthonormal principal axis. The strain plot, no longer bound to the horizontal axis except when isotropic, illustrates the necessity for aspectual strain. Here, vertical deviation from the tensile-compressive axis conveys the level of material orthotropy and in the same manner that the horizontal position of the circle centre indicates the state of dilatation strain, the vertical position is indicative of the maximum aspectual strain. Note that the horizontal skew plane increases with the *upwards* shear axis xy, and that vertical skew increases with the *downwards* shear axis yx.

An Eigen decomposition of the strain tensor yields eigenvalues λ_1, λ_2, λ_3, which represent the strain values for each principal orientation, and eigenvectors $[\mathbf{v}_1, \mathbf{v}_2, \mathbf{v}_3]^T$, which indicate the non-orthonormal principal axis. As a result, there no longer exists an orthogonal principal plane for any deviatoric stress state for the case of orthotropy. If infinitely orthotropic as in Figure 1, the absence of a Cartesian principal coordinate system is logically sound. Note that the conventional orthonormal principal values can be recovered by degeneration the OLST into the ILST by: $\left[\bar{\mathbf{v}} \quad \bar{\boldsymbol{\lambda}}\right] = \mathrm{eig}\left\{\left(\boldsymbol{æ} + \boldsymbol{æ}^{\mathrm{T}}\right)/2\right\}$.

3.3 The material stiffness matrix under strong orthotropy

The linear constitutive equation $æ_{ij} = S_{ijkl}\sigma_{kl}^{æ}$ utilises a generalised orthotropic compliance tensor, subsequent to the presented theory, having unique horizontal/vertical shear moduli

$$^{\{m\}}S_{ijkl} = \left\{\delta_{ik}\delta_{jl}\left(1+\nu_{ji}\right) - \delta_{ij}\delta_{kl}\nu_{lj}\right\}/E_l \tag{15}$$

where, the Poisson's ratio is $\nu_{ij} = -æ_{ii}/æ_{jj}$, and δ_{ij} is the Kronecker delta. For the plane stress condition the expanded nine-by-nine compliance tensor is truncated to give the required in-plane terms. This reduced matrix is inverted to yield the plane stress material stiffness matrix, $\mathbf{D}$, such that

$$\mathbf{D} = \begin{bmatrix} E_1/\left(1-\nu_{12}\nu_{21}\right) & \nu_{12}E_2/\left(1-\nu_{12}\nu_{21}\right) & \cdots 0 \cdots & \\ \nu_{21}E_1/\left(1-\nu_{12}\nu_{21}\right) & E_2/\left(1-\nu_{12}\nu_{21}\right) & & \\ \cdots 0 \cdots & & E_2/\left(1+\nu_{21}\right) & 0 \\ & & 0 & E_1/\left(1+\nu_{12}\right) \end{bmatrix} \tag{16}$$

For equivalence between the ILST and OLST, σ_{12}^{e} must equal $\sigma_{12}^{æ}$, where $()^{e}$ refers to the isotropic system representation, the conventional shear stiffness is found using the contraction rule:

$$\bar{D}_{1212} = 2D_{1212}D_{2121}/\left(D_{1212}+D_{2121}\right) \tag{17}$$

4 Numerical examples

4.1 Case study: Orthotropic trellis shear within a quasi corotational framework

A strongly orthotropic square element under a trellis-type deformation was used to demonstrate the effectiveness of the proposed tensors. This used a principal elastic modulus of 180 GPa, an orthogonal transverse modulus of one thousandth of this value, and a major Poisson's ratio of 0.4999. Its response is according to the constitutive model in (16) and related contraction by (17).

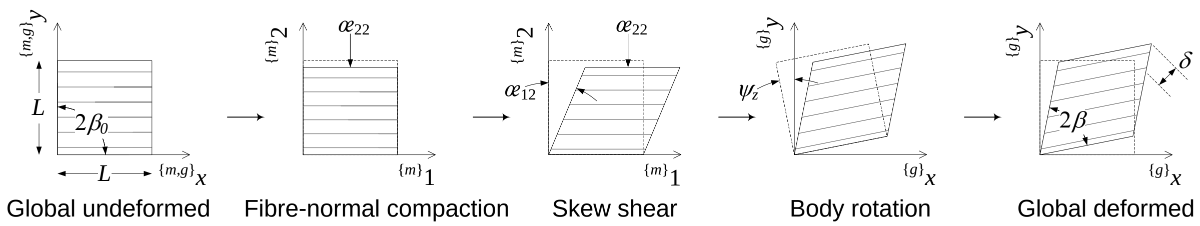

Figure 2. Effective treatment of an infinitely orthotropic material under trellis shear and plane stress

A benchmark analytical model was used, with the effective modality of Figure 2, which demonstrates a trellis motion whereupon side lengths remain constant. With displacement δ as a controlled input, the interior angle, and internal strains are kinematically determinate [5].

$$e_{11} = \sin\left\{2\cos^{-1}\left(\delta/2L + \cos\beta_0\right)\right\} - 1, \qquad e_{22} = 0, \qquad e_{12} = \sin\left\{2\beta_0 - 2\cos^{-1}\left(\delta/2L + \cos\beta_0\right)\right\}/2 \tag{18}$$

The NASTRAN code SOL101 was used to ascertain the second solution; although susceptible to second order rigid rotation, the example problem had no such geometric rotation. Using nonlinear geometry in the ANSYS code, the third solution was indifferent to rigid body rotation, including second order components, by way of Polar Decomposition: where the deformation gradient tensor $\mathbf{F}$ is decomposed into a rotation tensor $\mathbf{R}$ and the left stretch tensor $\mathbf{U}$ such that it satisfies: $\mathbf{F} = \mathbf{RU}$, where $\mathbf{F} = \bar{\nabla}\mathbf{u} + \mathbf{I}$. The nonlinear solver Marc was used to perform the fourth solution using the small strain and total Lagrangian formulation. Finally, the proposed OLST was used for an evaluation solution. As with the other iterative solvers, the linear first run returned an overly stiff solution, but also returned the distinct material principal rotation tensor. A subsequent run, $n+1$, used a simple implementation of co-rotation represented by $\mathbf{X}_{n+1} = \mathbf{Q}\mathbf{X}_n^{\mathrm{T}}$, where each fibre family was counter-rotated by a matrix $\mathbf{Q}$ using the angular value ψ_z. A similar process was repeated to recalculate the boundary displacements.

4.2 Results summary

Table 1. Comparison of solutions to a 1% trellis deformation of a simple square element under plane stress

Model	Strain (%)				Stress (MPa)		
	x	*y*	*xy*	*yx*	*x*	*y*	*xy*
Analytical	0	−2.020E−2	1.005	NA	−1.818E−2	−3.637E−2	3.611
NASTRAN SOL101	−5.051E−3	−5.051E−3	1.005	NA	−9.098	−1.364E−2	3.611
ANSYS NLGeom	−2.020E−2	→0	1.005	NA	−3.637E+1	−1.818E−2	3.611
Marc Total Lagr.	→0	→0	1.005	NA	→0	→0	3.611
Proposed OLST	−4.543E−8	−2.014E−2	2.007	3.009E−2	−1.821E−2	−3.626E−2	3.611

The results in Table 1 show the solutions from five possible procedures. In normal strain, whilst the error associated with the infinitely orthotropic analytical model is small, the entire planar compaction is directed to the fibre-normal axis. Meanwhile, the solution of NASTRAN is clearly incorrect as the result disregards material properties and hence does not model the deformation mode required for fibre inextensibility. The ANSYS solution, whilst rotationally insensitive, has a rotational basis measured against an arbitrary element edge or coordinate; thus it can be classified as being mesh dependent. In the Marc solution, by using material principal stretches, which after shearing are no longer orthogonal, the fibre inextensibility is reflected in the normal stresses producing a free shearing result. Critically though, the second-order fibre-normal compaction can no longer be seen in normal strain. Overall none of these conventional methods can reproduce the performance of the analytical model; and furthermore, that model is shown to be an approximation in comparison to the full implementation of the OLST with co-rotation. This final result, considered exact, identifies the fibre *near*-inextensibility, fibre-normal compaction, and the balance between these resulting from the finite orthotropic ratio.

The normal stress components of the analytical and proposed approaches indicate the small difference between an exact treatment and the approximated infinitely orthotropic treatment. The linear static solution shows a two to three order-of-magnitude locking in the fibre direction, while the ANSYS solution performed worse again. The normal stresses for Marc, approaching zero subject to numerical procedure (indicated by →0), were many orders of magnitude smaller than the correct values. Whilst being the best of the conventional solvers, it was clearly inferior to the proposed theory.

In shear strain, the results show all procedures produced the same total shear strain; however, clearly the presented theory is more informative in identifying the balance between the planar shear values. The distribution between these is approximately representative of the orthotropic ratio. In the results for shear stress, all values are equal, which suggests the proposed distribution of strains by the OLST is correct when used in comparison to a conventional shear modulus determined using (17). Overall, the proposed continuum mechanics approach provides the only solution with both a free-shearing response and the second order component due to fibre-normal compaction for any level of orthotropy.

5 Conclusions

A continuum mechanics theory that proposes a more informative and mechanistic metric of strain modes for strongly orthotropic materials has been presented. This is achieved through use of a material-property dependent and asymmetric strain tensor, and by the subsequently derived material principal rotation tensor. The theory has the capability to model the persistently orthotropic behaviour of all levels of orthotropy, and also reduces to conventional results when applied to isotropic materials. As a demonstration of the utility of the approach, a quasi-linear analysis of a trellis shear test was performed using various commercial codes to show the erroneous behaviour under finite shear deformation. These were compared to an analytical method based on the strongly orthotropic postulate and an implementation of the presented continuum mechanics solution. The results show the ability of the proposed approach to arrive at a solution more accurate as compared to the analytical or commercial solvers – and thus to be insusceptible to instances of erroneous response.

This work is a basis for continuing research aiming to create the theory and framework for the accurate prediction of forming of advanced composite materials. Further development requires the extension of this theory into a finite element formulation for plate and shell elements. This will require a more rigorous treatment in the nonlinear fields and the subsequent associated numerical methods.

Acknowledgements

This work was performed as part of the research program within the Cooperative Research Centre for Advanced Composite Structures (CRC-ACS). The authors acknowledge the support given by the CRC-ACS and UNSW, in particular Don Kelly, Xiaobo Yu, Rowan Paton, and research colleagues including Hou Man.

References

1. Cauchy, A.L., *Mémoire sur les systèmes isotropes de points materiels*. 1850: Institut National de France.
2. Green, G. and N.M. Ferrers, *Mathematical Papers of George Green*. 1970: Chelsea Pub Co.
3. Belytschko, T., W.K. Liu, and B. Moran, *Nonlinear finite elements for continua and structures*. 2000: Wiley New York.
4. Boisse, P., *Meso-macro approach for composites forming simulation.* Journal of Materials Science, 2006. **41**(20): p. 6591-6598.
5. Spencer, A.J.M., *Theory of fabric-reinforced viscous fluids.* Composites Part A: Applied Science and Manufacturing, 2000. **31**(12): p. 1311-1321.
6. Xue, P., X. Peng, and J. Cao, *A non-orthogonal constitutive model for characterizing woven composites.* Composites Part A: Applied Science and Manufacturing, 2003. **34**(2): p. 183-193.
7. Yu, X., et al., *Intra-ply shear locking in finite element analyses of woven fabric forming processes.* Composites Part A: Applied Science and Manufacturing, 2006. **37**(5): p. 790-803.
8. Nedjar, B., *An anisotropic viscoelastic fibre-matrix model at finite strains: Continuum formulation and computational aspects.* Computer Methods in Applied Mechanics and Engineering, 2007. **196**(9-12): p. 1745-1756.
9. Klinkel, S., C. Sansour, and W. Wagner, *An anisotropic fibre-matrix material model at finite elastic-plastic strains.* Computational Mechanics, 2005. **35**(6): p. 409-417.